

Focal Plane Quicklook

N. Ponthieu, F.-X. Désert, A. Benoît

December 21, 2011

1 Overview

We take the scan of Uranus of Oct. 18th, 2011 (scan 333) as a working example. After a median filter (201 samples window, i.e. 8.46s) of all the individual timelines, some channels show multiple images of the planet. We are still working on the best way to isolate each image of the planet automatically. Although we have several promising ways of doing it, they still require some manual tuning by the user. We will give update on this on-going work.

Let us assume that we have correctly identified each image for each kid and fitted a gaussian per image. We iteratively build a list of kids that have at least an image in common (e.g. Fig. 1). For simplicity, we will call such kids “brothers”. If the number of kids matches the number of images b_j , writing that each kid k_i sees a weighted sum of all its brothers, we solve

$$k_i = A_{ij}b_j \quad (1)$$

where the terms of A are the amplitudes of the gaussians that fit the images. This process separates brothers efficiently as can be seen on Fig. 1. In the following we will call “combined” a kid separated from its brothers.

Once we have separated all brothers, we can re-project the timelines and study beams and focal plane geometry a bit further.

2 Focal plane reconstruction

When sky observations are projected in (az,el) coordinates, the focal plane is rotated and distorted. We fit these effects and make channels correspond to focal plane pixels. We do this by looking for orthogonal rows and columns on the image. We have checked that using only kids without brothers nor artefacts or including combined ones as well did not change the result.

The distortion effect pointed out by Samuel Leclercq, although observed, does not hamper the first construction of the grid (see Fig. 2). An analytic description of this effect has been proposed by Samuel Leclercq. At this present day, we use polynomial 2D-fitting tools provided by IDL (`polywarp.pro`) and have not compared our results to Samuel’s expression. Results are presented on Figs. 2 and are satisfactory at this stage. They may be used as a tool to separate multiple images. For the sake of completeness, we show fits derived by `polywarp.pro` for different polynomial orders together with a figure of merit of the fit (Fig. 3). At this stage, we choose a degree of 4.

3 Some results and summary FITS file description

We give maps of beam widths in focal plane coordinates and of ellipticities on Figs. 4 and 5 for both matrices. Interpixel distances have been linearly magnified for clarity by a factor 4. A quantitative comparison has not been done yet with Robert Zylka’s reconstructions on Mars and Neptune [1]. We do however observe a broad agreement between his work and ours as far as pixel positions and beam width broadening towards the center of the FOV of the 1mm matrix are concerned.

These results of kid separation and focal plane reconstruction are summarized in a fits file. The location and name of this file (one file per scan configuration) is yet to be determined. The relevant lines of the header are presented in Tab. 1. Six values of `flag` have been defined for now and are explained in the header, along with a short description of coordinates conversion conventions and absolute calibration. In short, if `flag` is 1, the kid did not need any specific processing, if `flag` is 3, then the kid is the linear sum of the kids in `str.comp` with respective weights `str.coeff`. x_g and y_g are pixel coordinates on the focal plane whereas az_c and el_c are pixel centers in (az,el) coordinates referenced to those of pixel 0.

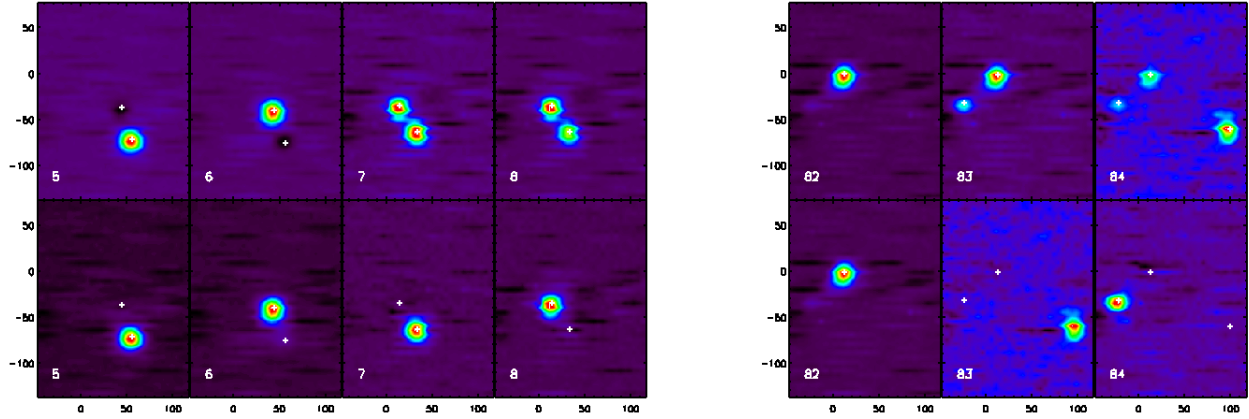


Figure 1: The timelines are median filtered by a window of 8.46 s (201 samples) and coadded into single channel maps. Channels 7 and 8 are coupled. Channel 84 shows a triple image (see below). Maps from Uranus scan 333, Oct. 18, 2011.

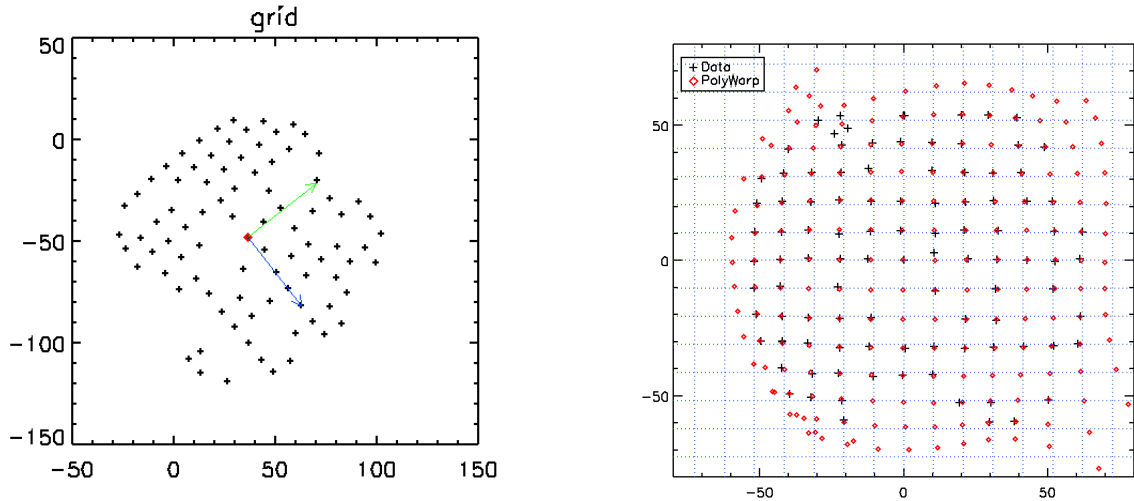


Figure 2: First figure: estimated beam centers in (az,el) coordinates. The two arrows represent the two orthogonal axes that minimize the difference between the observed grid and a regular orthogonal one. Second figure: Black crosses represent beam centers once rotated in focal plane coordinates ; red diamonds represent how the nodes of the grid (blue dotted lines) are distorted by the fitted polynomial. Apart for coupled detectors and a few outliers, the agreement with measured (black crosses) positions is excellent.

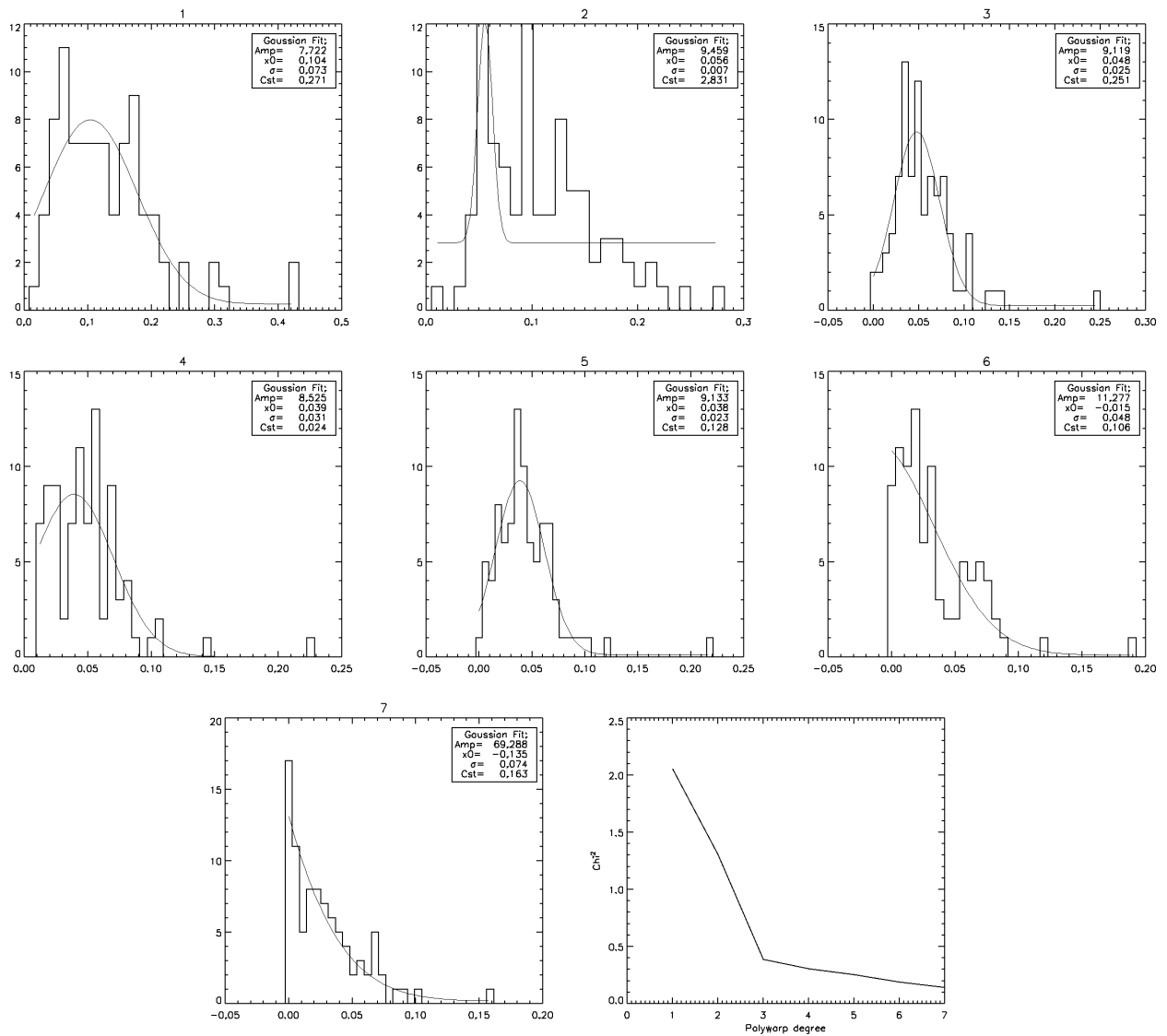


Figure 3: Histograms of the distance between measured beam positions and fit estimates using `polywarp.pro` for polynomial degrees varying from 1 to 7. The last plots gives a figure of merit of the fit quality : $\chi^2 = \sum (x - x_{fit})^2 + (y - y_{fit})^2$ as a function of the polynomial degree. 4 is satisfactory and corresponds to the order of Samuel's model.

XTENSION	= 'BINTABLE'	Binary table written by MWRFITS v1.11
BITPIX	= 8	Required value
NAXIS	= 2	Required value
NAXIS1	= 93	Number of bytes per row
NAXIS2	= 150	Number of rows
PCOUNT	= 0	Normally 0 (no varying arrays)
GCOUNT	= 1	Required value
TFIELDS	= 14	Number of columns in table
TTYPE1	= 'NAME '	
TTYPE2	= 'NUM '	
TTYPE3	= 'FLAG '	
TTYPE4	= 'XG '	
TTYPE5	= 'YG '	
TTYPE6	= 'AZ_C '	
TTYPE7	= 'EL_C '	
TTYPE8	= 'FWHM_X '	
TTYPE9	= 'FWHM_Y '	
TTYPE10	= 'THETA_DEG'	
TTYPE11	= 'COEFF '	
TTYPE12	= 'COMP '	
TTYPE13	= 'CALIB '	
TTYPE14	= 'MATRIX '	
TFORM1	= '6A '	
TFORM2	= 'I '	
TFORM3	= 'I '	
TFORM4	= 'I '	
TFORM5	= 'I '	
TFORM6	= 'D '	
TFORM7	= 'D '	
TFORM8	= 'D '	
TFORM9	= 'D '	
TFORM10	= 'D '	
TFORM11	= '3D '	
TFORM12	= '3I '	
TFORM13	= 'D '	
TFORM14	= 'A '	
MAGNIF_A	= 10.4136247282	
X0_A	= 36.1731879521	
Y0_A	= -47.7988595521	
ALPHA_A	= -0.910061860259	
FLUX_1MM	= 19.5300	[Jy]
FLUX_2MM	= 7.39000	[Jy]
COMMENT		flag = 0 : no signal
COMMENT		flag = 1 : good kid
COMMENT		flag = 2 : off resonance
COMMENT		flag = 3 : combination of several kids
COMMENT		flag = 4 : multiple beams, not separable
COMMENT		flag = 5 : strange resonance

Table 1: Extracted header of the focal plane description fits file.

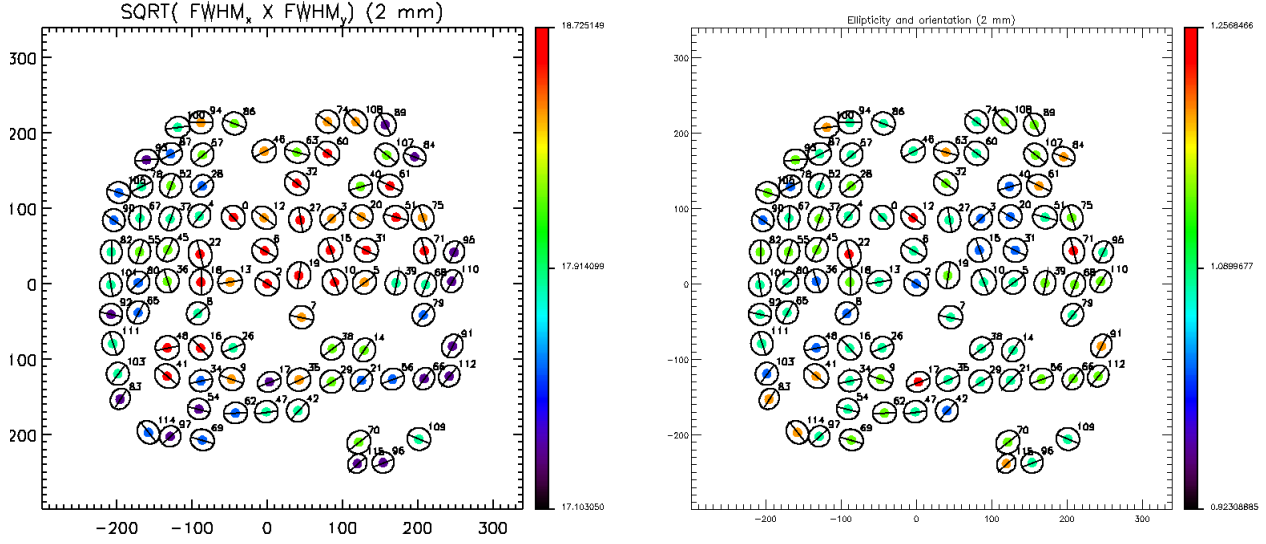


Figure 4: Each image provided by a given kid is fitted with an elliptical gaussian. Left: map of beam average FWHM derived from a gaussian elliptical fit. Colors scale like $FWHM = \sqrt{FWHM_x FWHM_y}$ on a $\pm 3\sigma$ range. The main axis of the ellipse is also represented for convenience. Right: map of ellipticity. We defined ellipticity such as $e = FWHM_x / FWHM_y$. We automatically call x the direction of maximum FWHM. The color scale drops below unity because we fix a $\pm 3\sigma$ range, but all ellipticities are larger than 1, according to their definition.

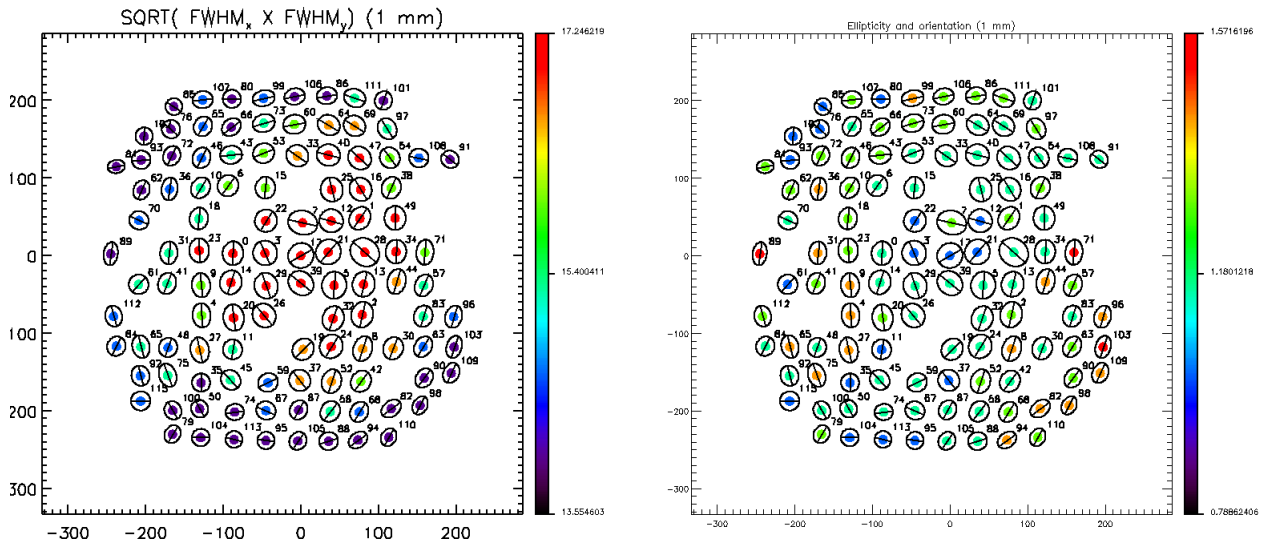


Figure 5: Same as Fig. 4 but for the 1mm matrix.

References

- [1] <http://www.iram.es/IRAMES/mainWiki/OffProcNika3>